



Photocatalytic degradation of three azo dyes using immobilized TiO₂ nanoparticles on glass plates activated by UV light irradiation: Influence of dye molecular structure

A.R. Khataee^{a,b,1}, M.N. Pons^{b,*}, O. Zahraa^{c,2}

^a Department of Applied Chemistry, Faculty of Chemistry, University of Tabriz, Tabriz, Iran

^b Laboratoire des Sciences du Génie Chimique, CNRS, Nancy Université, ENSIC, 1, rue Grandville, BP 20451, F-54001 Nancy Cedex, France

^c Département de Chimie-Physique des Réactions, INPL, Nancy Université, ENSIC, 1, rue Grandville, BP 451, F-54001 Nancy Cedex, France

ARTICLE INFO

Article history:

Received 26 November 2008

Received in revised form 9 February 2009

Accepted 10 February 2009

Available online 21 February 2009

Keywords:

TiO₂ nanoparticles

Photocatalysis

Electricity consumption

Azo dye

TOC

ABSTRACT

In order to discuss the effect of chemical structure on photocatalysis efficiency, the photocatalytic degradation of three commercial textile dyes (C.I. Acid Orange 10 (AO10), C.I. Acid Orange 12 (AO12) and C.I. Acid Orange 8 (AO8)) with different structure and different substitute groups has been investigated using supported TiO₂ photocatalyst under UV light irradiation. All the experiments were performed in a circulation photochemical reactor equipped with a 15-W UV lamp emitted around 365 nm. The investigated photocatalyst was industrial Millennium PC-500 (crystallites mean size 5–10 nm) immobilized on glass plates by a heat attachment method. SEM images of the immobilized TiO₂ nanoparticles showed the good coating on the plates, after repeating the deposition procedure three times. Our results indicated that the photocatalytic decolorization kinetics of the dyes were in the order of AO10 > AO12 > AO8. Photocatalytic mineralization of the dyes was monitored by total organic carbon (TOC) decrease, changes in UV–vis spectra and ammonium ion formation. The dye solutions could be completely decolorized and effectively mineralized, with an average overall TOC removal larger than 94% for a photocatalytic reaction time of 6 h. The nitrogen-to-nitrogen double bond of the azo dyes was transformed predominantly into NH₄⁺ ion. The kinetic of photocatalytic decolorization of the dyes was found to follow a first-order rate law. The photocatalysis efficiency was evaluated by figure-of-merit electrical energy per order (E_{EO}).

© 2009 Elsevier B.V. All rights reserved.

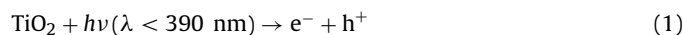
1. Introduction

Dyes are an abundant class of colored organic compounds that represent an increasing environmental danger. During dye production and textile manufacturing processes a large amount of wastewater containing dyestuffs with intensive color and toxicity can be introduced into aquatic systems. In most countries researchers are looking for appropriate treatments in order to remove pollutants, impurities and to obtain the decolorization of dyehouse effluents. Various chemical and physical processes, such as chemical precipitation and separation of pollutants, electrocoagulation [1,2], elimination by adsorption on activated carbon [3], etc., are currently used. One difficulty with these methods is that they are not destructive but only transfer the contamination from

one phase to another. Therefore, a new and different kind of pollution is faced and further treatments are deemed necessary [4–7]. Similarly conventional biological methods have not proven to be particularly effective for colored effluents. In most cases dyes are absorbed onto biomass without being really degraded [8,9]. Such pollution transfer is no more acceptable, as the sludge should be discarded in a sustainable manner.

In recent years as an alternative to conventional methods, “advanced oxidation processes” (AOPs), based on the generation of very reactive species such as hydroxyl radicals that have been proposed to oxidize quickly and non selectively a broad range of organic pollutants [9–11].

Heterogeneous photocatalysis via combination of TiO₂ and UV light is considered one of the promising advanced oxidation processes for destruction of water-soluble organic pollutants found in water and wastewater. When a light with $\lambda < 390$ nm is illuminating TiO₂ particles, an electron is excited out of its energy level and consequently leaves a hole in the valence band. Indeed, electrons are promoted from the valence band to the conduction band of TiO₂ to give electron–hole pairs (Eq. (1)) [12–15]:



* Corresponding author. Tel.: +33 3 83 17 52 77; fax: +33 3 83 17 53 26.

E-mail addresses: a.khataee@tabrizu.ac.ir (A.R. Khataee),

Marie-Noelle.Pons@ensic.inpl-nancy.fr (M.N. Pons),

Orfan.Zahraa@ensic.inpl-nancy.fr (O. Zahraa).

¹ Tel.: +98 411 3393165; fax: +98 411 3340191.

² Tel.: +33 3 83175118; fax: +33 3 83378120.

The valence band (h^+) potential is positive enough to generate hydroxyl radicals at the surface on TiO_2 and the conduction band (e^-) potential is negative enough to reduce molecular oxygen. The hydroxyl radical is a powerful oxidizing agent and attacks organic pollutants (P) present at or near the surface of TiO_2 . It causes, ultimately, complete decomposition of toxic and bioresistant compounds into harmless species such as CO_2 , H_2O , etc. [11,14,16,17].

In recent years, many investigations in the area of photocatalytic degradation of pollutants have employed suspensions of the semi-conducting particles. However, from a practical point of view it may not be possible to completely recover the photocatalysts used in the reactor [15,18]. This needs either long settling times or filtration which is an expensive process. Hence, many researchers have decided to study the feasibility of coating the photocatalyst on inert surfaces such as glass beads, activated carbon fiber, cotton material and cement surface [18–23]. Immobilization of the catalyst on a stationary support could circumvent the need to recover the catalyst from the reaction mixture without any leaching.

Another critical point in the study of photocatalytic processes efficiency towards dyes destruction is related to the complex nature of these pollutants. In a dyehouse they are mostly used as mixtures of dyes, formulated in function of the color to be created. The aim of the present work is to compare the photocatalytic destruction of three azo dyes (C.I. Acid Orange 10, C.I. Acid Orange 12 and C.I. Acid Orange 8) which exhibit small differences in their structure. The experiments were run in aqueous solution under UV light irradiation in the presence of supported TiO_2 . TiO_2 nanoparticles were immobilized on glass plates by a heat attachment method. In addition, ammonium production and total organic carbon removal were monitored in order to explain the mineralization of the dyes in the UV/ TiO_2 process.

2. Experimental

2.1. Materials

The dyes were obtained from Sigma–Aldrich Company and used without further purification. Their chemical structure and characteristics are given in Table 1. The investigated titanium dioxide was Millennium PC-500 (anatase: >99%). According to the manufacturer's specifications [24], the crystallites mean size was 5–10 nm and the specific surface area was $>300\text{ m}^2\text{ g}^{-1}$. The photocatalyst particles were deposited on $5\text{ cm} \times 28\text{ cm}$ glass plates from a suspension of TiO_2 .

2.2. Immobilization of TiO_2 on glass plates

TiO_2 nanoparticles were fixed on glass plates by a heat attachment method [18,25]. A suspension of Millennium PC-500 TiO_2 of 4 g l^{-1} in deionised water was prepared. The suspension concentration was chosen so as to get thin enough deposits. pH was adjusted to about 3 using diluted HNO_3 and the suspension was sonicated for 15 min (Bransonic 220, France). Then proper volume of suspension was carefully poured on the glass plates and allowed to dry out at room temperature for 12 h. Then the plates were completely dried out at 100°C for an hour. After drying, the plates were calcined at 475°C for 4 h. Before deposition, the glass surface was washed in a basic solution of NaOH in order to increase the number of OH groups. As shown in Fig. 1, the first coat is not covering the entire surface but additional coats lead to a complete coverage. Therefore, this deposition process was carried out three times in succession so as to increase the total thickness (Fig. 1). The plates were thoroughly washed with deionised water for the removal of free TiO_2 particles. The deposited amount of TiO_2 was measured by the difference in mass of the plates before and after immobilization.

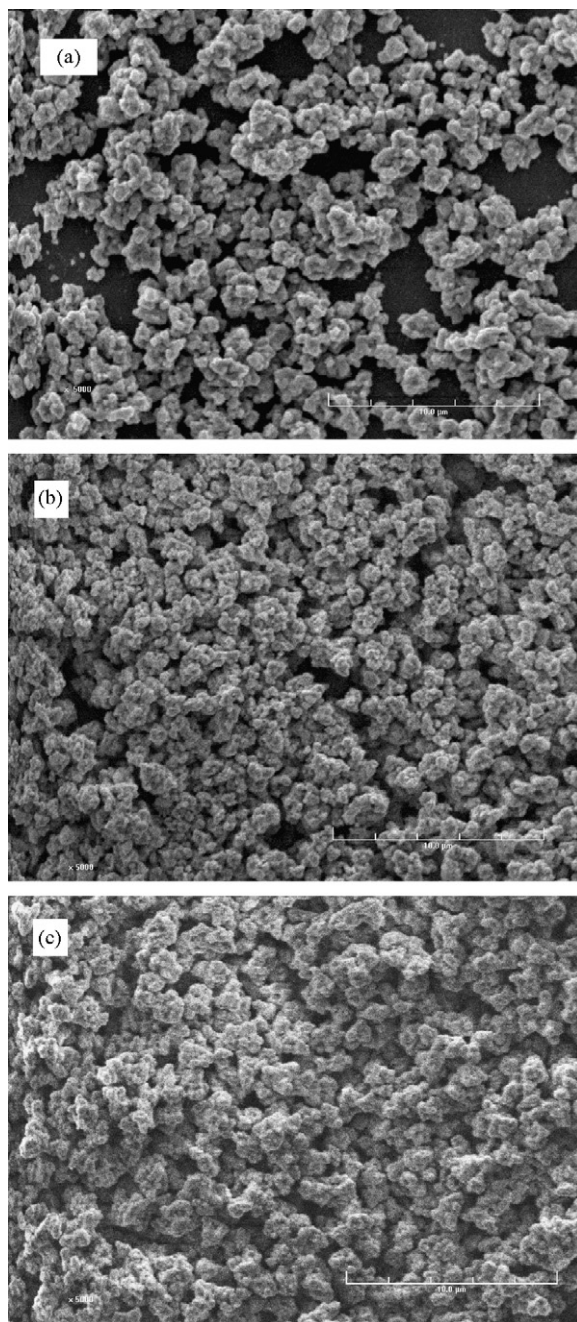


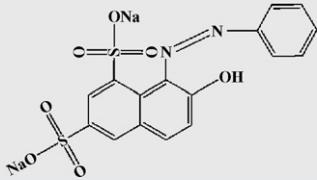
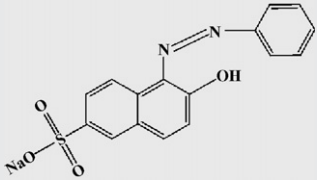
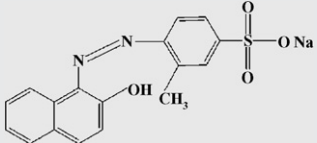
Fig. 1. Scanning electron microscopy images of TiO_2 nanoparticles deposited on glass plates: (a) first coat, (b) second coat, and (c) third coat. Bar = $10\ \mu\text{m}$.

Typically, the specific amount on TiO_2 in one coat was 0.47 mg/cm^2 . The photocatalysis of the dyes has been tested with these plates.

2.3. Photoreactor

The experimental set-up is based on a photocatalytic reactor of workable area $30\text{ cm} \times 30\text{ cm}$, made out of aluminium (Fig. 2) and covered by a thin layer of food-grade PTFE. The wastewater to be treated is falling as a thin film from the top of the chamber onto titanium dioxide nanoparticles immobilized on the six glass slides ($5\text{ cm} \times 28\text{ cm}$ each). A unique set of plates was used for all the experiments. The angle of slant was set at 37° to achieve a homogeneous distribution of the liquid. A transparent glass sheet covers the reacting chamber and permits to avoid the evaporation

Table 1
Structure and characteristics of the three commercial dyes.

Color index name	Chemical structure	Synonym	Molecular formula	Color index number	λ_{\max} (nm)	M_w (g mol ⁻¹)
C.I. Acid Orange 10 (AO10)		Orange G, Wool Orange 2G	C ₁₆ H ₁₀ N ₂ O ₇ S ₂ Na ₂	16230	480 (330)	452.4
C.I. Acid Orange 12 (AO12)		Crocein Orange G	C ₁₆ H ₁₁ N ₂ O ₄ Na	15970	488 (320)	350.3
C.I. Acid Orange 8 (AO8)		-	C ₁₇ H ₁₃ N ₂ O ₄ Na	15575	490 (310)	363.4

of the solution. The sample to be treated (250 ml of dye solution) was stored in a reservoir and was continuously circulated in the system by a peristaltic pump at a constant flow rate of 120 ml/min that permitted an optimal distribution of the liquid on the catalytic support. PTFE tubings were used. The reservoir was open to air to insure sufficient oxygenation. Artificial irradiation was provided by a 15-W UV lamp (Vilber Lourmat Deutschland GmbH, Eberhardzell, Germany) emitted around 365 nm, positioned parallel to the reactor. Light was turned on at the beginning of each experiment. The reactor was washed after every run by circulating deionised water with a few drops of 30% hydrogen peroxide under UV irradiation, so that the immobilized photocatalyst was regenerated. Adsorption measurements of the dyes on immobilized TiO₂ were made using the same set-up in the absence of irradiation.

2.4. Analytical procedures

The reactions were monitored by UV–vis spectrophotometer using a SECOMAM (Domont, France) Anthelie Light device in the range of 200–600 nm. A linear correlation was established between

the concentration of dyes (C) and the absorbance (A) at λ_{\max} , in the range of $C_{\text{dye}} = 0\text{--}50$ mg/l for each of the dyes. Total organic carbon (TOC) measurements were carried out by TOC analyser of Shimadzu TOC-VCSN (Japan). pH was measured using a PHM 220 pH meter (Radiometer Analytical SAS, Villeurbanne, France). The formation of NH₄⁺ after photocatalysis of the dye solutions was determined by Nessler method [26]. Scanning electron microscopy (SEM) was carried out on a Jeol TSM 330 device after gold plating of the samples.

3. Results and discussion

3.1. Adsorption of the dyes on the photocatalyst

As it was mentioned, the photocatalytic degradation takes place at the surface of the catalyst. Dye adsorbs on to the surface of TiO₂ by electrostatic attraction and gets mineralized by non-selective breakdown by hydroxyl radicals [27,28]. Therefore, the adsorption of the target molecule on the catalyst surface may be regarded as a critical step towards efficient photocatalysis. The study of adsorption of the dyes on immobilized TiO₂ revealed that, with a circulation rate of 120 ml/min, the equilibrium concentration was reached within about 60 min. The experiment was continued up to 90 min, but no significant change in the concentration was observed. Although the initial concentrations of the various dyes (C_0) were the same (30 mg/l), the equilibrium concentration (C_e) varied indicating different adsorption properties. The fraction of the dye adsorbed was expressed as adsorption (%) = $(C_0 - C_e)/C_0$ as illustrated in Fig. 3. C.I. Acid Orange 10, which has two sulphonate groups, exhibited a high adsorption yield (18%), which can be attributed to both the high molecular weight of this molecule compared to the other dyes, and the additional sulphonate group. In C.I. Acid Orange 10, due to its favorable dimension and spatial geometry, the $-\text{SO}_3^-$ can attach to surface Ti^{IV} centres by assuming a bidentate coordination through the two sulphonic oxygens. This process would be accompanied by substitution of a surface coordinated $-\text{OH}$ moieties. Because of the strong overlap between the 3d orbitals of the Ti^{IV} atoms and the 2p orbitals of oxygens, the formation of Ti–O bonds would have a strong covalent character [29,30].

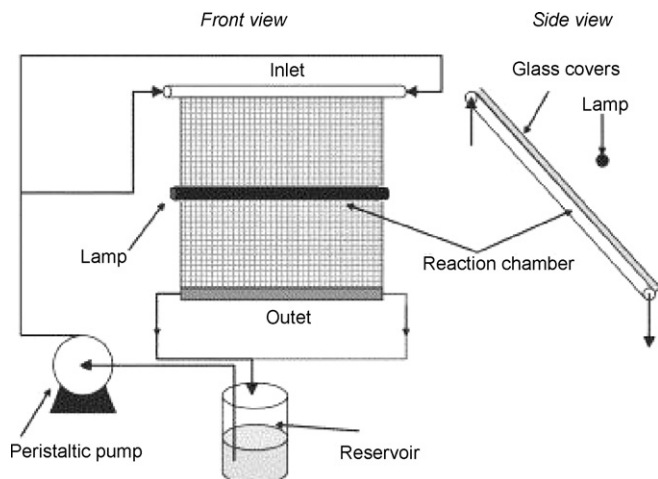


Fig. 2. Experimental set-up.

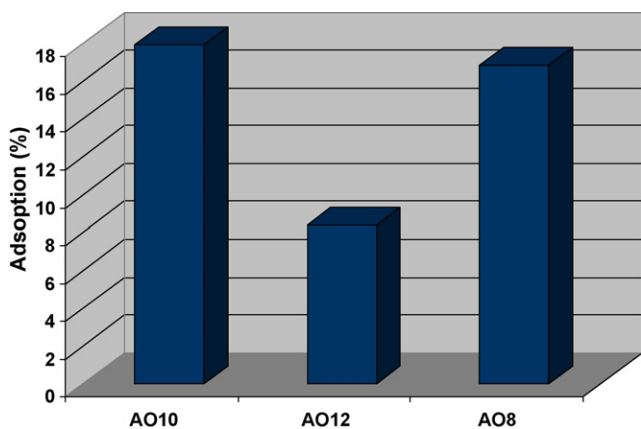


Fig. 3. Adsorption of the dyes on immobilized TiO₂. Experimental conditions: natural pH, [dye]₀ = 30 mg/l and time = 60 min.

AO8 and AO12 have nearly the same structure; the presence of the alkyl group (–CH₃) in the AO8 molecular structure can decrease slightly the adsorption of this dye. Hydroxyl radicals have a very short lifetime, so that they can only react where they are formed. Indeed, every group that tends to decrease the solubility of molecules in water will disfavor degradation. This explains, at least partly, why the adsorption efficiency of AO12 with a hydrophobic substituent clearly decreases [5].

3.2. Photocatalytic decolorization of the dyes

The changes in the absorption spectra of the three dyes during the photocatalytic process at different irradiation times are shown in Fig. 4. The color of an azo dye is the result of the interaction between an azo function (–N=N–) and two aromatic species: the dyes carry an acceptor group which is an aromatic nucleus frequently containing a chromophoric group, e.g. –SO₃[–], and a donor group, e.g. an aromatic nucleus containing an auxochromic group such as alkyl side chains, or OH group [5]. The decrease of absorption peaks of the dyes at the maximum absorption wavelength (λ_{max}) in Fig. 4 indicates a rapid decolorization of the azo dyes. The decrease is also meaningful with respect to the nitrogen-to-nitrogen double bond (–N=N–) of the azo dyes, as the most active site for oxidative attack. Decrease in absorption intensity of the band at λ_{max} during the irradiation also expresses the loss of conjugation, e.g. especially the cleavage near the azo bond of the organic molecule. The weak band at 310–330 nm could be attributed to the π–π* transition related to the aromatic ring attached to the –N=N– group in the dye molecule. Absorbance decrease at 310–330 nm indicates the degradation of aromatic part of the dyes [31].

The degradation pathway of the three dyes could be explained as follows: the fragile group in these dyes is the NH group, which results from an equilibrium between two tautomeric forms [21,25] where an H atom is exchanged between O and N as shown in Fig. 5 in the case of AO12. Indeed, the abstraction of H atom (carried by an oxygen atom in the azo form and by a nitrogen atom in the hydrazone form) by OH radicals is the main degradation pathway of these dyes. Meanwhile, the hydroxyl radical is an electrophilic entity, and the electronic properties of auxiliary groups will affect the electronic density in the aromatic nucleus and on the β nitrogen atom of the azo bond. Surprisingly, the presence of the more powerful electron withdrawing sulphonate group on a molecule makes it only very slightly less sensitive to oxidation [32]. Indeed, molecules with one or two sulphonic functions have almost the same reactivity with respect to oxidation by hydroxyl radicals (see Fig. 6). In fact, study of the influence of the sulphonate group is very difficult, because this substitute operates in different ways: on one

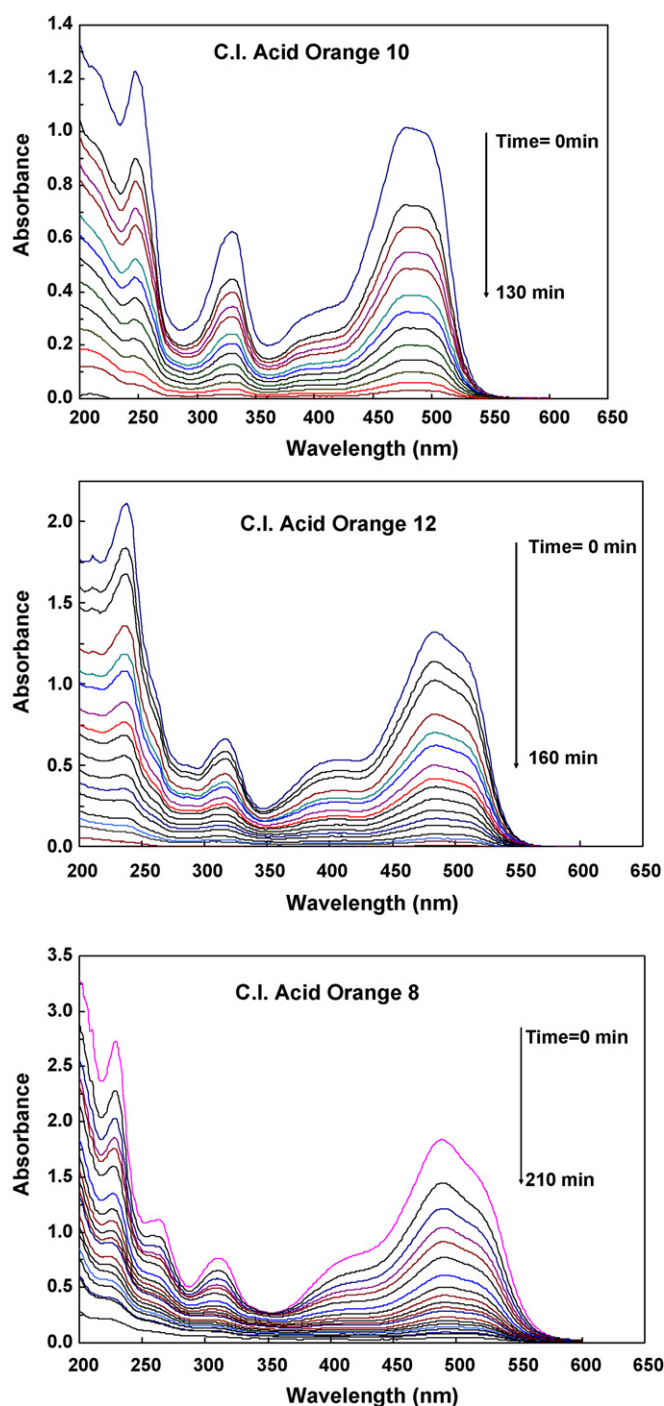


Figure 4. Variation of the absorbance of 30 mg/l aqueous solutions of the three azo dyes at different irradiation times. Experimental conditions: natural pH, [dye]₀ = 30 mg/l and sampling interval = 10 min.

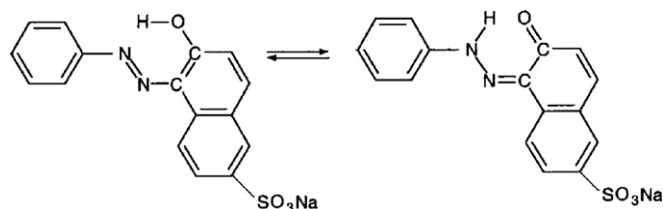


Fig. 5. Equilibrium between the two tautomeric forms in C. I. Acid Orange 12.

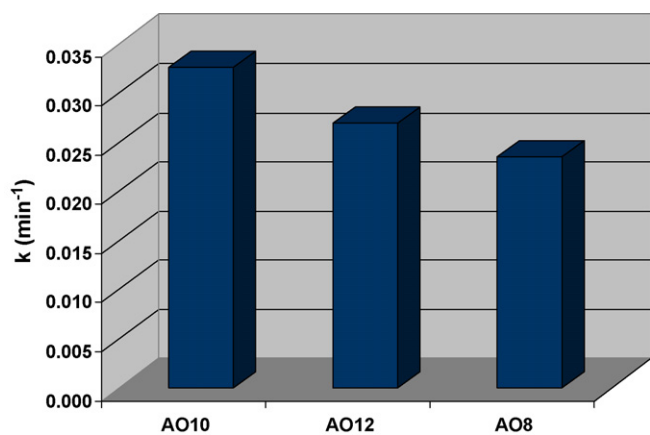


Fig. 6. Pseudo-first-order kinetic of the photocatalytic degradation of the dyes. Conditions: natural pH and $[dye]_0 = 30 \text{ mg/l}$.

hand it decreases electron density in the aromatic rings and the β nitrogen atom of the azo bond, but on the other hand, it increases the hydrophilic–lipophilic balance of the dye molecules, and as a consequence slows down their aggregation degree. The sulphonate group is also increasing the adsorption of the dye molecules on the catalyst. As it can be seen from Fig. 4, complete photodegradation of AO10 could be achieved in a relatively short time, 130 min, while, 160 and 210 min were taken for AO12 and AO8, respectively. Fig. 6 demonstrates that, in fact, the photodegradation kinetics notably depend upon the basic molecular structure of the dyes. According to Fig. 6, the photocatalytic degradation rates of the dyes are in the following order:

AO10 > AO12 > AO8

The presumed reason is that the adsorption rate of AO10 is higher than for the two other dyes because of two sulphonate groups and high molecular weight. Another reason may be due to absorption of light photon by dye molecule itself leading to a lesser availability of photons for hydroxyl radical generation. The absorption spectra of three dyes in UV range are shown in Fig. 7. It was observed from this figure that AO8 strongly absorb near UV radiation compared to AO12 and AO10 leading to lesser photodegradation. The above-mentioned order (AO10 > AO12 > AO8) was observed in absorption spectra of the three dyes in UV range. The strong absorption of light by the dye molecules is thought to have an inhibitive effect on the photogeneration of holes or hydroxyl radicals, because of the lack of any direct contact between the photons and immobilized TiO_2 . Indeed, it causes the dye molecules to adsorb light and the photons never reach the photocatalyst surface, thus the photodegradation efficiency decreases [27].

The recorded pH data during the experiments implied that at the end of the irradiation period the dye was degraded to small molecules, such as organic acids, since the pH dropped (Table 2).

3.3. Photocatalytic mineralization of the dyes

Mineralization of the dyes in UV/ TiO_2 process studied with 30 mg/l of each dye solutions. Mineralization was monitored by TOC loss, changes in UV spectra and also NH_4^+ evolution.

Table 2

Photocatalytic mineralization of the three commercial dyes at the irradiation time of 6 h, $[Dye]_0 = 30 \text{ mg/l}$.

Dye solution	Initial pH	Final pH	Potential amount of NH_4^+ (mg/l)	NH_4^+ (mg/l)	TOC removal (%)
AO10	6.41	5.20	1.91	0.338	97.96
AO12	6.09	5.13	2.15	0.282	96.89
AO8	6.86	5.60	1.92	0.327	94.47

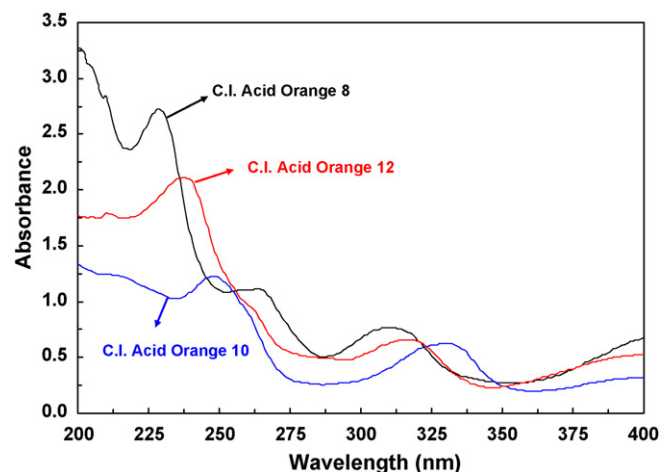


Fig. 7. UV absorption spectra of the three azo dyes (at 30 mg/l).

TOC values have been related to the total concentration of organics in the solution and the decrease of TOC reflects the degree of mineralization at the end of the photocatalytic process. TOC disappearance of the three azo dyes has been reported in Table 2. These results indicated that more than 94% TOC removal was achieved at the irradiation time of 6 h.

All of these dyes contain a source of nitrogen including an azo group (see Table 1). Previous works have shown that azo group is mainly transformed into ammonium ion and nitrogen gas N_2 , which is an ideal case for environment [25,32]. In this study we have only analysed ammonium ion. The evolution of NH_4^+ , as N-containing mineralization product during UV/ TiO_2 process is given in Table 2. A part of azo group present in these dyes may be transformed into N_2 as already observed in the degradation of other azo dyes [32–35]. These results indicate that ammonium is formed from azo group in the degradation of the dyes. The nitrogen-to-nitrogen double bond (R-N=N-R') belonging to the central aromatic rings of the dyes may be attacked by hydroxyl radical to transform into the two amino-groups (R-NH_2). The nitrogen atoms in these amino-groups can lead to NH_4^+ ions by successive attacks by H^\bullet atoms (Eqs. (2)–(4)). H^\bullet radicals can generate by photoreduction of protons (Eq. (4)) [32,35]:



3.4. Electrical energy determination

The plot of $\ln[Dye]$ versus irradiation time for the dyes was linear suggesting that the photocatalytic process approximately follows pseudo-first-order kinetics (Table 3). Rate constants were estimated from the slope of $\ln[Dye]$ versus time.

Since photocatalysis of aqueous organic pollutants is an electric energy intensive process, and electric energy can represent a major fraction of the operating costs, simple figures-of-merit based on electric energy consumption can be very useful and informative. Recently, the Photochemistry Commission of International Union of Pure and Applied Chemistry (IUPAC) has proposed two figures-

Table 3

The pseudo-first-order rate constant (k_1) and E_{EO} values for photocatalysis of the three commercial dyes, $[Dye]_0 = 30 \text{ mg/l}$.

Dye solution	k_1 (min^{-1})	R^2	E_{EO} (kWh m^{-3})
AO10	0.0326	0.90	70.67
AO12	0.0269	0.92	85.65
AO8	0.0235	0.97	98.04

of-merit for advanced oxidation processes (AOPs) on the use of electrical energy. In the zero-order range, the appropriate figure-of-merit is the electrical energy per mass (E_{Em}) defined as the kWh of electrical energy requires to remove 1 kg of the pollutant [36]. In the case of low pollutant concentrations, which applies here, the appropriate figure-of-merit is the electrical energy per order (E_{EO}), defined as the number of kWh of electrical energy required to reduce the concentration of a pollutant by one order of magnitude (90%) in 1 m^3 of contaminated water. The E_{EO} ($\text{kWh m}^{-3} \text{ order}^{-1}$) can be calculated from the following equations [37–39]:

$$E_{EO} = \frac{P \times t \times 1000}{V \times 60 \times \log(C_i/C_f)} \quad (5)$$

$$\ln(C_i/C_f) = k_1 \times t \quad (6)$$

where P is the rated power (kW) of the AOP system, t is the irradiation time (min), V is the volume (l) of the water in the reactor, C_i and C_f are the initial and final pollutant concentrations and k_1 is the pseudo-first-order rate constant (min^{-1}) for the decay of the pollutant concentration. From Eqs. (5) and (6), E_{EO} can be written as follows:

$$E_{EO} = \frac{38.4 \times P}{V \times k_1} \quad (7)$$

The electric energy (kWh m^{-3}) required to decolorization of 30 mg/l of the dyes from 250 ml dye solution has been given in Table 3. The E_{EO} values indicated that the required electrical energy for photocatalysis of these dyes was in the following order:

AO8 > AO12 > AO10

Finally, it is useful to relate the E_{EO} values found in this study to treatment costs. If the cost of the electricity, in the EU, is \$ 0.100 (taxes included) per kWh, the contribution to treatment cost from electrical energy will be \$ 7.1, 8.6, 9.8 per m^3 , for photocatalytic treatment of AO10, AO12 and AO8, respectively. In addition there will be small cost factors for the photocatalyst used and for UV lamp replacement.

4. Conclusion

The photodegradation of three monoazo anionic dyes from aqueous solution in the presence of immobilized TiO_2 nanoparticles under UV light irradiation was investigated. The commercially available catalyst with high photocatalytic activity (Millennium PC-500) was immobilized on comparatively inexpensive support substrates such as glass plates by heat attachment method. The results of TOC decrease, UV-vis spectra changes and formation of ammonium indicated that photocatalytic process could be used for complete decolorization and mineralization of the azo dyes in a circulation photochemical reactor. The attack of the $-\text{N}=\text{N}-$ azo group contributes to the decolorization of the dye solutions. The nitrogen-to-nitrogen double bond azo dye was transformed to NH_4^+ ion. The recorded pH data during the experiments implied that at the end of the irradiation period the dyes were degraded to small molecules, such as organic acids. The semi-log plot of the dye concentrations versus time was linear, suggesting first-order reaction. The electrical energy consumption for photocatalytic removal of the three dyes was calculated and related to the treatment costs. We found that

the electrical energy consumption was lowest with AO10 solution in comparison with AO8 and AO12 solutions.

Acknowledgments

The authors thank the University of Tabriz, Iran for financial support. We also sincerely thank Prof. Aleboeyeh, Mr Olya and Mr Kasiri (ENSCMu, Université de Haute Alsace, Mulhouse, France) for TOC analysis.

References

- [1] N. Daneshvar, A.R. Khataee, A.R. Amani Ghadim, M.H. Rasoulifard, Decolorization of C.I. Acid Yellow 23 solution by electrocoagulation process: investigation of operational parameters and evaluation of specific electrical energy consumption (SEEC), *J. Hazard. Mater.* 148 (2007) 566–572.
- [2] A. Alinsafi, M. Khemis, M.N. Pons, J.P. Leclerc, A. Yaacoubi, A. Benhammou, A. Nejmeddine, Electro-coagulation of reactive textile dyes and textile wastewater, *Chem. Eng. Process.* 44 (2005) 461–470.
- [3] N. Daneshvar, S. Aber, A. Khani, A.R. Khataee, Study of imidaclopride removal from aqueous solution by adsorption onto granular activated carbon using an on-line spectrophotometric analysis system, *J. Hazard. Mater.* 144 (2007) 47–51.
- [4] Y.M. Slokar, A.M.L. Marechal, Methods of decoloration of textile wastewaters, *Dyes Pigments* 37 (1998) 335–356.
- [5] C. Galindo, P. Jacques, A. Kalt, Photooxidation of the phenylazonaphthol AO20 on TiO_2 : kinetic and mechanistic investigations, *Chemosphere* 45 (2001) 997–1005.
- [6] N. Daneshvar, A.R. Khataee, D. Salari, A. Niaei, Photocatalytic degradation of the herbicide erioglucine in the presence of nanosized titanium dioxide: comparison and modeling of reaction kinetics, *J. Environ. Sci. Heal. B* 41 (2006) 1273–1290.
- [7] O. Tunay, I. Kabdasli, G. Eremektar, D. Orhon, Color removal from textile wastewaters, *Water Sci. Technol.* 34 (1996) 9–16.
- [8] F.I. Hai, K. Yamamoto, K. Fukoshi, Hybrid treatment systems for dye wastewater, *Crit. Rev. Environ. Sci. Technol.* 37 (2007) 315–377.
- [9] T. Sano, E. Puzenat, C. Guillard, C. Geantet, S. Matsuzawa, Degradation of C_2H_2 with modified- TiO_2 photocatalysts under visible light irradiation, *J. Mol. Catal. A-Chem.* 284 (2008) 127–133.
- [10] A.R. Khataee, V. Vantanpour, A.R. Amani, Decolorization of C.I. Acid Blue 9 solution by UV/Nano- TiO_2 , Fenton, Fenton-like, electro-Fenton and electro-coagulation processes: a comparative study, *J. Hazard. Mater.* 161 (2009) 1225–1233.
- [11] M. Kitano, M. Matsuoka, M. Ueshima, M. Anpo, Recent developments in titanium oxide-based photocatalysts, *Appl. Catal. A-Gen.* 325 (2007) 1–14.
- [12] K. Pirkanniemi, M. Sillanpaa, Heterogeneous water phase catalysis as an environmental application: a review, *Chemosphere* 48 (2002) 1047–1060.
- [13] T. Yates Jr., T.L. Thompson, Surface science studies of the photoactivation of TiO_2 -new photochemical processes, *Chem. Rev.* 106 (2006) 4428–4453.
- [14] A. Fujishima, X. Zhang, Titanium dioxide photocatalysis: present situation and future approaches, *C.R. Chimie* 9 (2006) 750–760.
- [15] A. Alinsafi, F. Evenou, E.M. Abdulkarim, M.N. Pons, O. Zahraa, A. Benhammou, A. Yaacoubi, A. Nejmeddine, Treatment of textile industry wastewater by supported photocatalysis, *Dyes Pigments* 74 (2007) 439–445.
- [16] X. Chen, S.S. Mao, Titanium dioxide nanomaterials: synthesis, properties, modifications and applications, *Chem. Rev.* 107 (2007) 2891–2959.
- [17] J.M. Herrmann, Heterogeneous photocatalysis: state of the art and present applications, *Top. Catal.* 34 (2005) 49–65.
- [18] N. Daneshvar, D. Salari, A. Niaei, M.H. Rasoulifard, A.R. Khataee, Immobilization of TiO_2 nanopowder on glass beads for the photocatalytic decolorization of an azo dye C.I. Direct Red 23, *J. Environ. Sci. Heal. A* 40 (2005) 1605–1617.
- [19] M. Lackhoff, X. Prieto, N. Nestle, F. Dehn, R. Niessner, Photocatalytic activity of semiconductor-modified cement-influence of semiconductor type and cement ageing, *Appl. Catal. B-Environ.* 43 (2003) 205–216.
- [20] M.A. Behnajady, N. Modirshahla, M. Mirzamohammady, B. Vahid, B. Behnajady, Increasing photoactivity of titanium dioxide immobilized on glass plate with optimization of heat attachment method parameters, *J. Hazard. Mater.* 160 (2008) 508–513.
- [21] B. Tryba, Immobilization of TiO_2 and Fe-C- TiO_2 photocatalysts on the cotton material for application in a flow photocatalytic reactor for decomposition of phenol in water, *J. Hazard. Mater.* 151 (2008) 623–627.
- [22] H. Huang, G. Huang, H. Chen, Y. Lee, Immobilization of TiO_2 nanoparticles on Fe-filled carbon nanocapsules for photocatalytic applications, *Thin Solid Films* 515 (2006) 1033–1037.
- [23] B. Neppolian, H.C. Choi, S. Sakthivel, B. Arabindoo, V. Murugesan, Solar/UV-induced photocatalytic degradation of three commercial textile dyes, *J. Hazard. Mater.* 89 (2002) 303–317.
- [24] Millennium Inorganic Chemicals, Certificated Analysis, PC 500 Lot No. 6293000124, 2007.
- [25] O. Zahraa, C. Dorion, S.M. Ould-Mame, M. Bouchy, Titanium dioxide deposit films for photocatalytic studies of water pollutants, *J. Adv. Oxid. Technol.* 4 (1999) 40–46.

- [26] Standard Methods for the Examination of Water and Wastewater, by American Public Health Association, American Water Works Association, Water Environment Federation, 4500-NH₃ Nitrogen (Ammonia), 1999.
- [27] R.A. Damodar, K. Jagannathan, T. Swaminathan, Decolorization of reactive dyes by thin film immobilized surface photoreactor using solar irradiation, *Sol. Energ.* 81 (2007) 1–7.
- [28] S. Malato, J. Blanco, J. Caceres, A.R. Fernandez-Alba, A. Aguera, A. Rodriguez, *Catal. Today* 76 (2002) 209–220.
- [29] R. Comparelli, E. Fanizza, M.L. Curri, P.D. Cozzoli, G. Mascolo, R. Passino, A. Agostiano, Photocatalytic degradation of azo dyes by organic-capped anatase TiO₂ nanocrystals immobilized onto substrates, *Appl. Catal. B-Environ.* 55 (2005) 81–91.
- [30] C. Bauer, P. Jacques, A. Kalt, Investigation of the interaction between a sulfonated azo dye (AO7) and a TiO₂ surface, *Chem. Phys. Lett.* 307 (1999) 397–406.
- [31] N.H. Ince, M.I. Stefan, J.R. Bolton, UV/H₂O₂ degradation and toxicity reduction of textile dyes: remazol black-B, a case study, *J. Adv. Oxid. Technol.* 2 (1997) 442–448.
- [32] H. Lachheb, E. Puzenat, A. Houas, M. Ksibi, E. Elaloui, C. Guillard, J.M. Herrmann, Photocatalytic degradation of various types of dyes (Alizarin S, Crocein Orange G, Methyl Red, Congo Red, Methylene Blue) in water by UV-irradiated titania, *Appl. Catal. B-Environ.* 39 (2002) 75–90.
- [33] M. Karkmaz, E. Puzenat, C. Guillard, J.M. Herrmann, Photocatalytic degradation of the alimentary azo dye amaranth: mineralization of the azo group to nitrogen, *Appl. Catal. B-Environ.* 51 (2004) 183–194.
- [34] T.H. Bui, M. Karkmaz, E. Puzenat, C. Guillard, J.M. Herrmann, Solar purification and potabilization of water containing dyes, *Res. Chem. Intermediat.* 33 (2007) 421–431.
- [35] K. Sahel, N. Perol, H. Chermette, C. Bordes, Z. Derriche, C. Guillard, Photocatalytic decolorization of Remazol Black 5 (RB5) and Procion Red MX-5B-Isotherm of adsorption, kinetic of decolorization and mineralization, *Appl. Catal. B-Environ.* 77 (2007) 100–109.
- [36] J.R. Bolton, K.G. Bircger, W. Tumas, C.A. Tolman, Figure-of merit for the technical development and application of advanced oxidation technologies for both electric- and solar-derived systems, *Pure Appl. Chem.* 73 (2001) 627–637.
- [37] N. Daneshvar, A. Aleboyeh, A.R. Khataee, The evaluation of electrical energy per order (EEo) for photooxidative decolorization of four textile dye solutions by the kinetic model, *Chemosphere* 59 (2005) 761–767.
- [38] C. Stephen, M.I. Stefan, J.R. Bolton, A. Safarzadeh-Amiri, UV/H₂O₂ treatment of methyl tert-butyl ether in contaminated waters, *Environ. Sci. Technol.* 34 (2000) 659–662.
- [39] A. Safarzadeh-Amiri, O₃/H₂O₂ treatment methyl-tert-butyl ether in contaminated waters: effect of background COD on the O₃-dose, *Ozone Sci. Eng.* 24 (2002) 55–62.